

Contents of this file

Part S1: The water-rock interaction process of EAFZ groundwaters are simulated by PHREEQC software.

Part S2: Supplementary Figures

Figure S1. Cl-SO₄-HCO₃ ternary diagram (Giggenbach, 1991)

Figure S2. Statistical Figure of trace elements (B, Al, Ba, Li, Ra and Sr). Literature data from (Aydin et al., 2020; Baba et al., 2019; Okan et al., 2018; Yuce et al., 2014; Pasvanoglu, 2020).

Figure S3. Spider diagram of the water in the EAFZ. Enrichment coefficients (weight ratios) normalized by Ti. $EF_i = (C_i/C_{Ti})_w / (C_i/C_{Ti})_r$, where i is element, w is water, r is rock. Rocks chemistry are taken from (Nurlu, 2020).

Part S3: Supplementary Tables

Table S1 Chemical and hydrogen and oxygen isotopic compositions of EAFZ groundwater, 2013-2023. Data source: (Aydin et al., 2020; Baba et al., 2019; Okan et al., 2018; Yuce et al., 2014; Pasvanoglu, 2020; Yasın and YÜce, 2023; Karaoğlu et al., 2019).

Table S2 Temperature results obtained with empirical chemical geothermometers (values in °C) and depths (km) of origin for EAFZ groundwaters.

Part S4. Videos:

Video. 1 Seismic precursor anomaly of HS14 geothermal fluid. Shooting time: A month before the earthquake.

Video. 2 Post-earthquake anomaly of HS04 geothermal fluid. Shooting time: March 26th, 2023.

Part S1:

PHREEQC is a powerful water chemistry simulation software. In this study, we used its function to simulate “Irreversible Reactions” (Parkhurst and Appelo, 2013).

Mineral data preparation

The proportion of minerals in water-rock reaction was calculated by CIPW (Cross, Iddings, Pirsson, Washington) (Table P1-1 and P1-2). The calculated data were from Karaoğlu et al. (2020).

Table P1-1 Results of CIPW calculation

Mineral	Quartz	Plagioclase	Orthoclase	clinopyroxene	orthopyroxene	Ilmenite	Hematite	Apatite	Sphene
content wt%	6.1	58	13.12	3.59	6.28	0.28	8.36	0.86	3.42

Table P1-2 Results of standardization of minerals associated with water-rock reaction

Mineral	Plagioclase	Orthoclase	pyroxene
content wt%	58	13.12	9.87
standardization %wt	0.72	0.16	0.12

Note: The minerals involved in the water-rock reaction are mainly plagioclase, potassium feldspar and pyroxene, and the three minerals are re-standardized according to 100%. Pyroxene is the sum of two kinds of pyroxene.

PHREEQC simulation step (Table P1-3)

Choose Databases: `llnl.dat`

`SOLUTION_SPREAD` setup:

HS08 is a river sample, and the initial simulated water sample is defined as the chemical composition of HS08. The initial temperature is 53°C, which is the thermal reservoir temperature of the river water estimated by SiO₂.

`EQUILIBRIUM_PHASES` setup:

Italiano et al. (2013) reported that the carbon dioxide volume fraction of EAFZ ranges from 88.4% to 99.9%. Therefore, the initial CO₂ percentage is set as 88.4%, and the logarithm is 1.95.

REACTION setup: We set up 6 groups of reactants mixed in different proportions respectively, as shown in Table P1-4:

Table P1-3 PHREEQC code and description

Steps	Instructions
SOLUTION_SPREAD -units mg/l Temperature pH Si Li Na K Mg Ca F Cl Br N(5) S(6) HCO3 B Al Mn Fe Sr Ba Zn as SiO2 as NO3 as SO4 53 8.43 15.15 1.00E-06 1.13 1.00E-06 4.47 55.34 0.4411 1.06 1.00E-06 3.83 5.69 165.72358 0.00477 0.01227 0.00105 0.01252 0.05578 0.00189 0.01899	Initial reactant input (HS08)
EQUILIBRIUM_PHASES 1 CO2(g) 0 1.95	Equilibrium phases setting
Reaction 1 NaCl 1 0.07 moles	Deep fluid mixing ratio setting
save solution 1 end use solution 1	Store the mixed solution
REACTION 2 Calcite 1 Anhydrite 0.3 albite 0.4 Anorthite 0.4 Ca-Al_Pyroxene 0.1 K-feldspar 0.16 Dolomite 1	Water rock reaction mineral Settings
1 moles in 20 steps	Reaction steps and total amount of reaction

Table P1-4 The proportion of minerals added

	Mineral	content	Albite	Anorthite	Calcite	Dolomite	Anhydrite	Orthoclase	pyroxene
R1		0%	0.7	0.02	0.4	0.4	0	0.16	0.12
R2	deep fluid	2%		0.02	0.4	0.4	0	0.16	0.12
R3	(NaCl)	5%		0.02	0.4	0.4	0	0.16	0.12
R4		7%		0.02	0.4	0.4	0	0.16	0.12
R5	Water-rock reaction	30%	0.4	0.4	1	1	0.3	0	0
R6	(Anhydrite)	100%	0	0	0	0	1	0	0

The total amount of reaction was set to 1mol, and the reaction was carried out in 20 steps. The simulation results are shown in Table P1-5.

Table P1-5 Simulation results of water-rock interaction in the EAFZ by PHREEQC.

step	2%NaCl						5%NaCl						7%NaCl					
	Ca ²⁺	SO ₄ ²⁺	HCO ₃ ⁻	Cl ⁻	HCO ₃ ⁻ +Cl ⁻	Na ⁺	Ca ²⁺	SO ₄ ²⁺	HCO ₃ ⁻	Cl ⁻	HCO ₃ ⁻ +Cl ⁻	Na ⁺	Ca ²⁺	SO ₄ ²⁺	HCO ₃ ⁻	Cl ⁻	HCO ₃ ⁻ +Cl ⁻	Na ⁺
	mol/L						mol/L						mol/L					
Mix	1.37	0.05	0.00	0.03	0.03	0.05	1.37	0.05	0.00	0.03	0.03	0.05	1.37	0.05	0.00	0.03	0.03	0.05
0	1.37	0.05	0.14	19.96	20.10	19.98	1.37	0.05	0.14	49.67	49.81	49.69	1.37	0.05	0.14	69.38	69.52	69.40
1	32.88	0.03	54.65	19.83	74.48	51.82	33.34	0.03	54.56	49.41	103.97	79.96	33.61	0.03	54.47	69.04	123.51	98.67
2	58.52	0.02	82.68	19.81	102.49	83.42	58.91	0.02	82.37	49.36	131.73	111.03	59.16	0.02	82.15	68.99	151.14	129.39
3	79.54	0.02	103.91	19.81	123.72	114.52	79.93	0.02	103.48	49.37	152.85	141.75	80.17	0.02	103.19	69.01	172.19	159.85
4	97.70	0.02	120.72	19.82	140.54	145.23	98.08	0.02	120.20	49.40	169.60	172.14	98.32	0.02	119.85	69.04	188.89	190.03
5	113.76	0.02	134.27	19.83	154.10	175.59	114.13	0.02	133.68	49.43	183.11	202.23	114.38	0.02	133.28	69.09	202.37	219.93
6	128.21	0.02	145.28	19.85	165.12	205.64	128.58	0.02	144.63	49.47	194.09	232.01	128.81	0.02	144.19	69.14	213.33	249.54
7	141.37	0.02	154.23	19.86	174.09	235.38	141.73	0.02	153.53	49.50	203.03	261.51	141.96	0.02	153.07	69.19	222.26	278.87
8	153.46	0.02	161.47	19.88	181.35	264.83	153.81	0.02	160.74	49.54	210.27	290.72	154.04	0.02	160.26	69.23	229.49	307.92
9	164.65	0.02	167.27	19.89	187.16	293.98	165.00	0.02	166.51	49.57	216.08	319.64	165.23	0.02	166.01	69.27	235.28	336.68
10	175.09	0.02	171.83	19.90	191.73	322.83	175.43	0.02	171.05	49.59	220.65	348.26	175.66	0.02	170.54	69.31	239.85	365.15
11	184.86	0.02	175.31	19.91	195.22	351.38	185.21	0.02	174.52	49.62	224.14	376.58	185.43	0.02	174.00	69.34	243.33	393.31
12	194.07	0.02	177.85	19.92	197.77	379.62	194.41	0.02	177.05	49.63	226.68	404.59	194.64	0.02	176.52	69.36	245.88	421.17
13	202.77	0.02	179.55	19.92	199.48	407.54	203.12	0.02	178.75	49.64	228.39	432.28	203.34	0.02	178.22	69.36	247.58	448.70
14	211.04	0.02	180.51	19.92	200.44	435.13	211.38	0.02	179.71	49.64	229.35	459.63	211.60	0.02	179.18	69.36	248.54	475.89
15	218.91	0.02	180.81	19.92	200.73	462.37	219.25	0.02	180.01	49.63	229.64	486.63	219.48	0.02	179.49	69.34	248.83	502.74
16	226.43	0.01	180.52	19.91	200.43	489.26	226.78	0.01	179.73	49.61	229.34	513.27	227.00	0.01	179.21	69.31	248.52	529.21
17	233.65	0.01	179.69	19.90	199.60	515.77	233.99	0.01	178.92	49.57	228.49	539.53	234.22	0.01	178.41	69.26	247.67	555.31
18	240.59	0.01	178.39	19.89	198.28	541.88	240.94	0.01	177.63	49.53	227.16	565.40	241.16	0.01	177.13	69.20	246.33	581.00
19	247.29	0.01	176.66	19.87	196.52	567.59	247.64	0.01	175.92	49.47	225.39	590.84	247.86	0.01	175.43	69.11	244.55	606.27
20	253.77	0.01	174.54	19.84	194.38	592.87	254.12	0.01	173.82	49.40	223.23	615.86	254.35	0.01	173.35	69.01	242.36	631.11

Continued

step	0NaCl						100%Anhydrite						30%Anhydrite					
	Ca ²⁺ mol/L	SO ₄ ²⁺	HCO ₃ ⁻	Cl ⁻	HCO ₃ ⁻ +Cl ⁻	Na ⁺	Ca ²⁺ mol/L	SO ₄ ²⁺	HCO ₃ ⁻	Cl ⁻	HCO ₃ ⁻ +Cl ⁻	Na ⁺	Ca ²⁺ mol/L	SO ₄ ²⁺	HCO ₃ ⁻	Cl ⁻	HCO ₃ ⁻ +Cl ⁻	Na ⁺
Mi _x	1.37	0.05	0.00	0.03	0.03	0.05	1.37	0.05	0.00	0.03	0.03	0.05	1.37	0.05	0.00	0.03	0.03	0.05
0	1.37	0.05	0.13	0.03	0.16	0.05	1.37	0.05	0.13	0.03	0.16	0.05	1.37	0.05	0.13	0.03	0.16	0.05
1	32.54	0.03	54.66	0.03	54.69	33.02	11.65	10.15	0.18	0.03	0.21	0.05	48.90	5.80	57.42	0.03	57.45	17.96
2	58.24	0.02	82.88	0.03	82.91	64.96	20.50	18.96	0.21	0.03	0.24	0.05	87.36	10.35	83.94	0.03	83.97	35.12
3	79.27	0.02	104.19	0.03	104.22	96.31	28.87	27.31	0.23	0.03	0.26	0.05	123.16	14.32	106.78	0.03	106.81	51.90
4	97.43	0.02	121.06	0.03	121.09	127.23	36.95	35.37	0.24	0.03	0.27	0.05	156.98	17.86	126.90	0.03	126.93	68.34
5	113.51	0.02	134.66	0.03	134.69	157.78	44.81	43.22	0.25	0.03	0.28	0.05	189.21	21.03	144.87	0.03	144.90	84.44
6	127.96	0.02	145.71	0.03	145.74	188.00	52.50	50.89	0.26	0.03	0.29	0.05	220.13	23.88	161.05	0.03	161.08	100.20
7	141.12	0.02	154.69	0.03	154.72	217.91	60.02	58.41	0.27	0.03	0.30	0.05	249.91	26.45	175.67	0.03	175.70	115.62
8	153.22	0.02	161.96	0.03	161.99	247.51	67.42	65.79	0.28	0.03	0.31	0.04	278.19	28.79	188.27	0.03	188.30	130.71
9	164.42	0.02	167.78	0.03	167.81	276.82	74.68	73.04	0.29	0.03	0.31	0.04	303.36	31.01	196.77	0.03	196.80	145.49
10	174.85	0.02	172.35	0.03	172.38	305.82	81.83	80.18	0.29	0.03	0.32	0.04	325.51	33.13	201.38	0.03	201.41	159.99
11	184.63	0.02	175.84	0.03	175.87	334.52	88.87	87.22	0.30	0.03	0.33	0.04	345.87	35.10	203.73	0.03	203.75	174.23
12	193.84	0.02	178.39	0.03	178.42	362.92	95.81	94.15	0.30	0.03	0.33	0.04	365.03	36.91	204.61	0.03	204.64	188.20
13	202.54	0.02	180.09	0.03	180.12	390.99	102.64	100.98	0.31	0.03	0.34	0.04	383.29	38.57	204.42	0.03	204.45	201.90
14	210.80	0.02	181.05	0.03	181.08	418.73	109.39	107.72	0.31	0.03	0.34	0.04	400.83	40.06	203.39	0.03	203.42	215.34
15	218.68	0.02	181.35	0.03	181.38	446.13	116.05	114.38	0.32	0.03	0.35	0.04	417.75	41.40	201.66	0.03	201.69	228.50
16	226.20	0.02	181.05	0.03	181.08	473.18	122.62	120.94	0.32	0.03	0.35	0.04	434.15	42.59	199.35	0.03	199.38	241.38
17	233.41	0.01	180.21	0.03	180.24	499.85	129.11	127.43	0.32	0.03	0.35	0.04	450.09	43.63	196.56	0.03	196.59	253.97
18	240.35	0.01	178.90	0.03	178.93	526.14	135.52	133.84	0.33	0.03	0.36	0.04	465.62	44.53	193.35	0.03	193.38	266.26
19	247.05	0.01	177.15	0.03	177.18	552.02	141.86	140.17	0.33	0.03	0.36	0.04	480.80	45.30	189.78	0.03	189.81	278.25
20	253.53	0.01	175.02	0.03	175.05	577.47	148.12	146.42	0.33	0.03	0.36	0.04	495.66	45.93	185.91	0.03	185.94	289.93

Part S2:

Figure S1. Cl-SO₄-HCO₃ ternary diagram (Giggenbach, 1991)

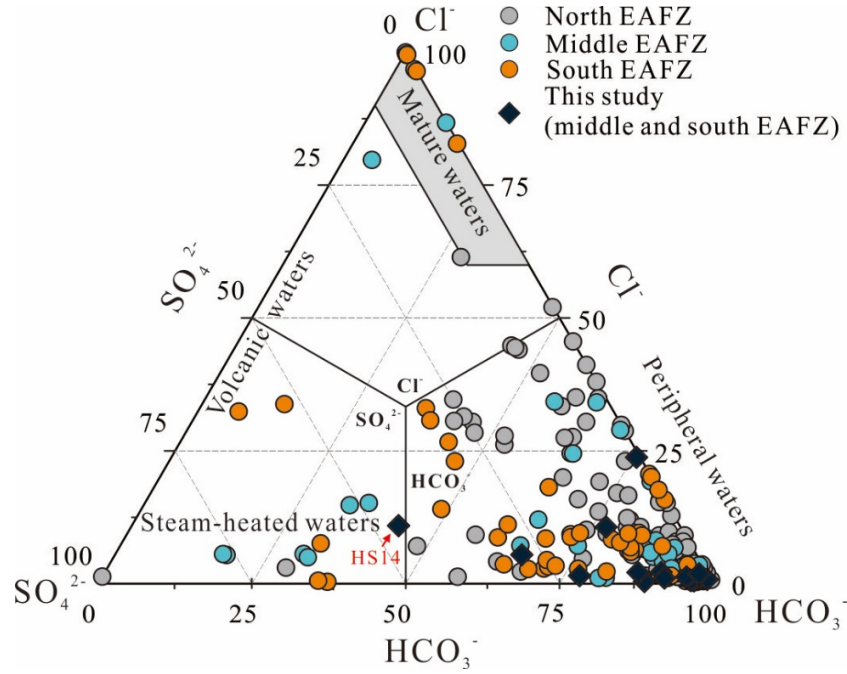


Figure S2. Statistical Figure of trace elements (B, Al, Ba, Li, Ra and Sr). Literature data from (Aydin et al., 2020; Baba et al., 2019; Okan et al., 2018; Yuce et al., 2014; Pasvanoglu, 2020).

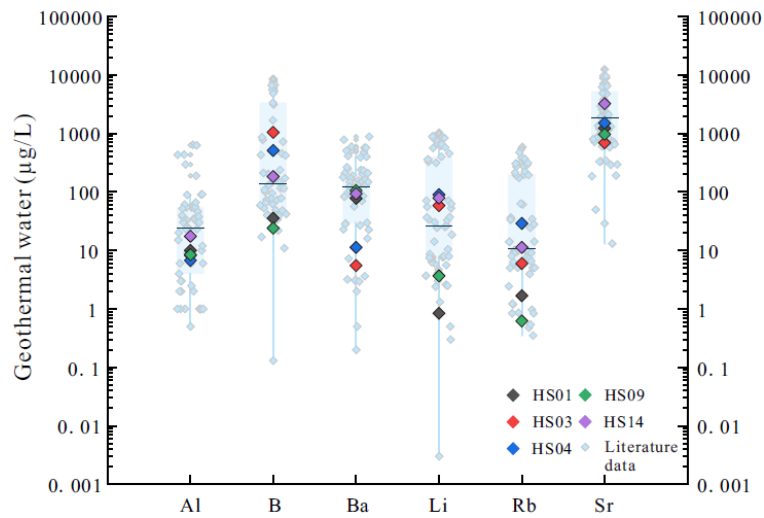
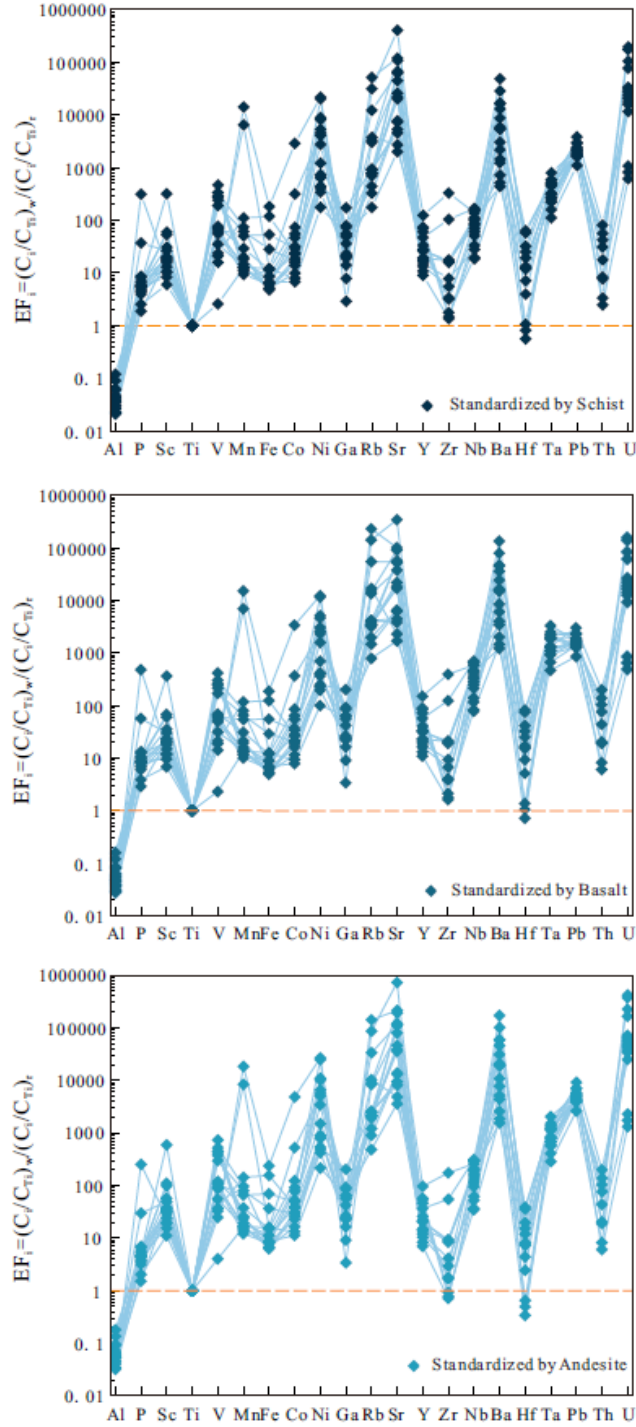


Figure S3. Spider diagram of the water in the EAFZ. Enrichment coefficients (weight ratios) normalized by Ti. $EF_i = (C_i/C_{Ti})_w / (C_i/C_{Ti})_r$, where i is element, w is water, r is rock. Rocks chemistry are taken from (Nurlu, 2020).



Part S3:

Table S1 Chemical and hydrogen and oxygen isotopic compositions of EAFZ groundwater, 2013-2023

T	pH	Na ⁺	K ⁺	Ca ²⁺	Mg ²⁺	HCO ₃ ⁻	Cl ⁻	SO ₄ ²⁻	SiO ₂	δ ¹⁸ O	δD	Data source
(°C)		mg/L	mg/L	mg/L	mg/L	mg/L	mg/L	mg/L	mg/L			
63.2	6.8	1050.0	140.0	410.0	82.0	3100.0	460.0	290.0	150.0	-12.5	-96.0	Aydin H., Karakuş H. and Mutlu H. (2020) Hydrogeochemistry of geothermal waters in eastern Turkey: Geochemical and isotopic constraints on water-rock interaction. Journal of Volcanology and Geothermal Research 390.
18.7	7.8	3.3	0.8	11.0	1.3	41.0	0.7	4.8	3.5	-12.7	-86.0	
55.1	9.7	39.0	0.9	13.0	0.4	83.0	2.8	37.0	79.0	-14.2	-99.0	
5.5	7.4	1.3	0.3	6.2	0.5	25.0	0.4	1.1	2.7	-13.9	-94.0	
32.5	7.2	40.0	0.7	31.0	0.1	47.0	4.9	110.0	50.0	-14.0	-95.0	
17.5	7.9	2.6	0.4	22.0	2.1	76.0	0.4	3.4	8.2	-13.1	-89.0	
11.7	5.3	314.0	19.0	240.0	45.0	1100.0	150.0	230.0	120.0	-13.7	-96.0	
13.1	7.0	6.5	5.2	43.0	7.1	150.0	4.5	13.0		-13.1	-93.0	
36.6	5.6	2050.0	51.0	370.0	64.0	3000.0	1750.0	240.0	120.0	-13.4	-104.0	
6.0	7.3	4.7	0.5	9.0	2.9	47.0	0.5	2.1	6.0	-12.1	-82.0	
15.2	6.0	48.0	8.5	33.0	33.0	370.0	9.0	6.1	68.0	-13.3	-93.0	
17.4	6.8	46.0	8.2	36.0	33.0	350.0	9.0	8.5		-13.1	-92.0	
36.1	9.4	130.0	1.4	18.0	1.6	160.0	79.0	63.0	62.0	-14.5	-101.0	
9.2	7.4	20.0	0.6	25.0	9.0	150.0	4.8	3.3		-10.0	-66.0	
24.3	5.9	1600.0	20.0	260.0	170.0	2500.0	1750.0	2.5	120.0	-12.7	-93.0	
14.7	7.6	5.1	1.5	15.0	5.1	81.0	1.1	1.5		-11.9	-80.0	
11.6	5.6	160.0	13.0	260.0	150.0	1400.0	180.0	110.0	110.0	-13.6	-100.0	
27.0	6.1	1100.0	46.0	260.0	78.0	3050.0	320.0	150.0	100.0	-10.1	-84.0	
11.9	8.0	42.0	3.6	41.0	21.0	290.0	6.1	21.0	6.9	-12.7	-92.0	
36.5	6.1	2400.0	73.0	220.0	88.0	5950.0	660.0	160.0	140.0	-10.5	-88.0	
57.3	7.3	2550.0	82.0	290.0	130.0	6700.0	590.0	150.0	120.0	-10.7	-88.0	
14.5	7.2	16.0	3.2	51.0	29.0	310.0	4.1	9.6	18.0	-11.2	-77.0	

24.9	5.7	240.0	34.0	120.0	51.0	950.0	140.0	4.7	80.0	-13.8	-98.0
13.1	7.5	16.0	3.8	31.0	13.0	190.0	2.5	4.0	6.1	-13.1	-94.0
37.7	6.3	1800.0	59.0	520.0	160.0	2300.0	2500.0	5.2	180.0	-13.2	-97.0
28.6	6.3	710.0	53.0	240.0	120.0	1550.0	950.0	0.2	100.0	-12.2	-91.0
12.5	7.1	10.0	4.2	39.0	7.5	160.0	3.4	8.1	7.5	-11.0	-75.0
57.0	6.6	900.0	120.0	450.0	240.0	2850.0	1150.0	0.3	170.0	-12.5	-92.0
13.6	6.1	30.0	6.5	72.0	37.0	440.0	7.3	12.0	7.5	-12.8	-92.0
28.5	5.9	460.0	17.0	82.0	96.0	1400.0	250.0	0.1	100.0	-13.1	-91.0
12.9	7.3	16.0	1.6	20.0	9.6	140.0	5.6	1.8		-12.5	-84.0
33.4	6.2	450.0	21.0	93.0	100.0	1600.0	160.0	2.3	140.0	-13.0	-90.0
11.6	7.2	17.0	1.2	21.0	10.0	140.0	1.1	5.3		-12.9	-88.0
36.0	6.2	1700.0	42.0	150.0	81.0	2150.0	1800.0	0.8	110.0	-13.3	-95.0
38.4	6.5	1500.0	40.0	160.0	100.0	2700.0	1150.0	0.4	140.0	-13.6	-97.0
19.2	7.9	1300.0	17.0	61.0	15.0	3500.0	25.0	0.0	68.0	-12.5	-94.0
14.5	7.4	14.0	1.1	75.0	27.0	360.0	2.7	7.0	5.3	-11.0	-77.0
33.4	6.5	570.0	19.0	420.0	600.0	4050.0	770.0	37.0	180.0	-12.3	-90.0
18.6	5.9	80.0	8.4	67.0	330.0	1900.0	36.0	60.0	110.0	-12.2	-84.0
13.7	7.5	2.1	0.7	2.1	43.0	210.0	2.9	12.0		-11.7	-82.0
25.3	6.5	190.0	9.9	510.0	52.0	1950.0	170.0	20.0	51.0	-12.0	-82.0
30.3	6.4	86.0	21.0	230.0	110.0	1400.0	65.0	53.0	80.0	-12.0	-78.0
46.9	6.6	84.0	14.0	160.0	60.0	950.0	64.0	32.0	95.0	-12.2	-79.0
41.0	6.5	46.0	10.0	240.0	70.0	1150.0	19.0	44.0	75.0	-12.0	-76.0
24.6	6.4	770.0	46.0	150.0	110.0	1800.0	560.0	68.0	85.0	-12.1	-87.0
19.5	5.4	22.0	34.0	49.0	9.3	130.0	19.0	120.0	86.0	-14.0	-96.0
48.3	7.0	160.0	70.0	93.0	81.0	880.0	160.0	140.0	68.0	-12.6	-94.0
64.2	6.6	120.0	52.0	130.0	84.0	920.0	120.0	100.0	153.0	-11.3	-91.0
53.7	7.0	160.0	59.0	180.0	69.0	990.0	120.0	160.0	60.0	-11.5	-92.0

25.8	2.4	34.0	71.0	70.0	32.0	0.0	9.0	670.0	140.0	-10.8	-79.0	
50.6	7.2	170.0	69.0	69.0	76.0	590.0	180.0	130.0	56.0	-12.5	-95.0	
65.2	6.6	160.0	76.0	130.0	52.0	710.0	270.0	120.0	120.0	-12.8	-90.0	
39.8	6.9	150.0	70.0	78.0	78.0	750.0	170.0	150.0	79.0	-12.8	-94.0	
11.5	7.8	17.0	1.9	48.0	30.0	310.0	1.0	8.2	5.2	-12.9	-91.0	
18.1	6.2	180.0	20.0	92.0	12.0	400.0	190.0	34.0	45.0	-11.4	-83.0	
65.0	6.5	1850.0	190.0	330.0	64.0	1150.0	2500.0	420.0	78.0	-10.1	-79.0	
51.1	7.1	730.0	70.0	220.0	75.0	1200.0	640.0	460.0	57.0	-11.3	-82.0	
37.0	7.0	610.0	170.0	200.0	30.0	1600.0	360.0	150.0	100.0	-11.4	-90.0	
25.8	6.1	240.0	77.0	52.0	50.0	750.0	160.0	53.0	130.0	-12.2	-85.0	
34.3	7.6	84.0	24.0	99.0	71.0	810.0	17.0	23.0	130.0	-13.5	-91.0	
25.1	6.7	380.0	120.0	140.0	170.0	1950.0	160.0	63.0	130.0	-11.6	-85.0	
11.4	7.2	10.0	0.7	20.0	2.8	85.0	1.0	6.3	23.0	-12.1	-83.0	
53.5	7.6	2600.0	170.0	180.0	69.0	5500.0	850.0	540.0	99.0	-3.4	-72.0	
25.4	6.7	40.0	4.3	180.0	120.0	1150.0	14.0	40.0	19.0	-12.7	-89.0	
34.0	7.2	900.0	160.0	110.0	120.0	2100.0	560.0	260.0	31.0	-10.7	-82.0	
46.8	9.2	210.0	4.2	20.0	1.5	210.0	140.0	110.0	31.0	-10.9	-72.0	
16.3	6.3	140.0	26.0	390.0	190.0	1200.0	27.0	850.0	11.0	-10.7	-69.0	
51.6	6.9	320.0	33.0	70.0	15.0	1100.0	23.0	0.4	170.0	-9.6	-65.0	
14.2	10.4	120.0	13.0	100.0	62.0	900.0	32.0	4.2	9.0	-9.8	-66.0	
34.5	6.5	300.0	52.0	130.0	94.0	1550.0	47.0	0.5	120.0	-10.0	-69.0	
11.6	6.2	6.3	2.4	25.0	7.8	110.9	2.6	4.4		-10.6	-65.9	Karaoğlu Ö., Bazargan M., Baba A. and Browning J. (2019) Thermal fluid circulation around the Karlioia triple junction: Geochemical features and volcano-tectonic implications (Eastern
29.0	6.0	970.0	77.2	218.7	177.4	1971.7	1077.0	38.7				
26.8	6.1	335.3	30.4	100.4	83.5	1139.0	208.9	15.3		-12.5	-82.5	
22.5	6.2	269.1	25.8	189.5	182.7	2069.7	77.3	0.9		-12.5	-78.5	
28.2	5.8	269.0	31.0	115.2	118.1	1391.9	102.9	11.9		-12.2	-79.8	
8.9	7.7	3.9	0.8	26.5	2.7	89.3	0.6	1.6				

8.6	7.1	2.6	1.1	7.1	2.1	33.9	0.3	0.9				Turkey). Geothermics 81, 168-184.
32.0	6.1	225.1	34.0	200.7	131.4	1688.3	37.4	20.1	-12.5	-80.4		
14.8	6.2	22.1	6.1	90.8	50.5	533.0	3.5	9.5				
11.0	6.5	5.7	1.9	15.7	5.6	77.0	0.8	1.5				
10.3	6.5	4.1	2.3	14.9	4.5	73.9	1.1	2.0				
7.2	6.7	2.7	1.2	13.2	2.5	58.6	0.3	0.8				
9.2	6.7	4.1	1.3	13.3	4.4	70.9	0.5	1.5				
9.2	6.9	3.7	1.4	16.1	3.6	67.8	0.6	1.7				
6.7	7.1	2.6	1.6	8.5	2.4	36.9	0.5	2.0				
4.9	7.3	2.4	1.1	7.1	2.1	33.8	0.2	0.8				
7.5	7.1	4.8	1.0	12.7	2.6	58.5	0.4	1.6				
13.2	5.4	52.8	18.6	84.3	27.5	499.1	4.1	6.4				
6.0	7.3	3.2	1.4	7.5	2.1	36.9	0.3	0.9				
5.4	6.4	2.6	1.3	8.1	1.6	33.9	0.3	1.0				
27.0	6.0	142.0	24.4	392.0	571.0	2928.0	117.0	1076.0	144.0	-6.1	-31.6	
27.2	6.3	144.0	24.2	473.0	597.0	2891.0	116.0	1211.0	135.5			YasİN D. and YÜCe G.
27.2	6.3	148.0	25.8	493.0	552.0	2902.0	131.0	1023.0	141.0	-5.7	-30.0	(2023) Isotope and
31.5	6.4	247.0	39.9	705.0	542.0	3373.0	191.0	1695.0	152.1	-6.2	-33.2	hydrochemical
22.0	6.3	42.4	7.4	172.0	573.0	3142.0	49.1	219.0	118.4	-5.7	-27.4	characteristics of thermal
19.3	6.2	3.7	0.8	561.0	183.0	763.0	7.1	1287.0	40.5	-6.5	-32.4	waters along the active fault
19.6	6.0	7.5	1.6	548.5	167.1	781.0	12.6	1408.0	37.7	-6.2	-35.0	zone (Erzin-Hatay/Turkey)
21.3	6.2	15.6	0.6	169.0	173.0	1226.0	19.9	81.3	65.2	-4.4	-24.3	and their geothermal
23.3	11.4	1353.0	69.0	57.7	0.0	390.0	1903.0	5.8	1.9	-4.3	-26.0	potential. Turkish Journal
13.0	7.1	3.2	1.2	39.3	10.6	95.0	6.3	50.0	24.0	-11.7	-77.0	of Earth Sciences 32, 721-
52.0	6.3	998.0	91.2	207.0	70.5	1755.0	764.0	250.0	122.0	-10.3	-77.0	739.
67.0	6.2	766.0	69.3	116.0	47.8	1342.0	593.0	225.0	120.0	-11.1	-80.0	
64.0	6.2	1062.0	93.6	144.0	23.7	1800.0	1026.0	245.0	79.0	-10.5	-79.0	Pasvanoglu S. (2020)
												Geochemistry and
												conceptual model of
												thermal waters from Erzis -

59.0	6.9	220.0	105.0	110.0	53.5	1400.0	90.0	175.0	128.0	-10.2	-79.0	Zilan Valley, Eastern Turkey. Geothermics 86.
64.0	7.0	738.0	105.0	121.0	19.0	1154.0	878.0	185.0	90.0	-10.4	-79.0	
78.0	5.1	750.0	68.0	160.0	8.0	875.0	750.0	540.0	90.0			
64.0	6.3	838.0	99.0	135.0	14.0	1075.0	1075.0	250.0	90.0			
65.0	6.5	850.0	88.0	150.0	12.0	1000.0	950.0	208.0	80.0	-10.2	-80.0	
65.0	6.5	875.0	86.0	150.0	12.0	1000.0	975.0	219.0	80.0			
20.0	6.4	71.0	8.4	32.0	12.0	252.0	15.6	62.0	27.0			
80.0	7.9	830.0	74.0	96.0	56.0	994.0	715.0	565.0	109.0			
92.0	7.5	773.0	110.0	36.9	54.6	897.0	543.0	470.0	95.0			
98.0	7.7	858.0	108.0	29.5	47.0	779.0	560.0	491.0	118.0			
14.0	8.0	20.0	3.2	17.0	9.7	80.0	13.0	48.0	15.0	-11.9	-84.0	
37.1	7.1	270.6	51.4	592.9	104.0	2593.4	131.0	174.5				
38.4	6.6	285.5	58.4	591.8	106.2	2635.7	155.0	178.8				
37.8	6.5	280.7	52.2	615.4	103.4	2676.8	134.0	176.8				
24.5	6.2	22.0	3.6	191.7	24.7	577.6	8.0	119.3				
29.4	6.3	192.8	45.6	406.7	69.4	1731.4	110.0	130.0				
44.5	6.5	323.2	88.7	573.7	114.1	2523.1	260.0	199.4				Öztekin Okan Ö., Kalender L. and Çetindağ B. (2018) Trace-element hydrogeochemistry of thermal waters of Karakoçan (Elazığ) and Mazgirt (Tunceli), Eastern Anatolia, Turkey. Journal of Geochemical Exploration 194, 29-43.
44.6	6.5	340.6	69.5	629.4	114.9	2857.9	200.0	191.8				
30.7	6.3	163.8	41.3	321.9	62.1	1416.9	99.0	117.3				
19.0	6.4	387.1	56.4	140.0	132.5	1769.0	166.0	107.2				
13.1	5.8	13.4	1.7	99.3	8.6	345.1	8.0	8.0				
14.5	5.9	21.7	3.2	90.4	15.6	369.8	12.0	11.0				
13.2	6.1	19.6	3.3	106.4	10.2	392.9	10.0	8.0				
12.6	6.0	20.5	2.0	57.9	11.0	240.4	18.0	7.8				
12.8	6.8	52.7	4.1	106.6	21.3	512.3	15.0	23.5				
11.3	6.0	27.0	4.2	147.5	10.0	522.7	13.0	17.5				
14.3	6.1	32.1	6.3	123.0	15.3	488.7	14.0	14.1				

12.0	6.4	9.9	1.9	98.6	13.6	356.3	5.0	13.8				
37.7	6.2	254.2	62.6	514.5	105.1	2349.2	156.0	180.7				
38.0	6.7	288.7	74.5	584.5	116.5	2731.6	136.0	178.5				
38.0	6.8	257.7	62.9	370.2	107.4	1930.0	146.0	178.0				
24.7	6.8	20.1	3.3	176.3	25.1	531.5	7.0	119.0				
27.9	6.2	198.4	43.2	342.0	72.5	1599.5	92.0	131.4				
45.0	6.5	351.0	84.4	607.5	118.4	2925.2	141.0	192.2				
44.4	6.5	344.8	81.3	600.1	117.4	2852.5	135.0	193.7				
30.0	6.4	172.2	37.4	315.7	64.7	1449.0	98.0	121.2				
19.5	6.4	417.1	63.6	595.1	157.9	3329.6	121.0	105.0				
14.6	6.4	10.9	1.6	97.3	8.7	338.3	7.0	8.5				
15.2	6.5	20.5	3.0	92.5	16.3	378.3	11.0	11.0				
13.3	6.5	12.7	3.8	103.0	9.2	375.7	6.0	4.9				
13.8	5.9	21.1	1.8	56.9	11.5	240.8	15.0	12.0				
18.1	6.7	45.9	2.8	104.8	21.8	481.8	13.0	19.0				
15.1	6.2	21.2	5.0	148.8	9.8	522.7	9.0	10.0				
16.7	7.1	71.8	7.3	128.3	14.5	609.9	11.0	14.0				
12.8	6.3	16.1	1.7	103.0	14.9	402.8	8.0	6.3				
14.5	10.5	3.5	0.3	14.9	1.7	1.8	12.0	0.0	1.5	-6.8	-48.2	Baba A., Şaroğlu F., Akkuş I., Özel N., Yeşilnacar M. İ., Nalbantçılar M. T., Demir M. M., Gökçen G., Arslan Ş., Dursun N., Uzelli T. and Yazdani H. (2019) Geological and hydrogeochemical properties of geothermal systems in the southeastern region of Turkey. Geothermics 78, 255-271.
22.5	11.7	77.2	2.7	66.9	0.0	0.0	66.9	0.0	0.2	-7.9	-45.4	
27.8	8.2	12.5	3.9	45.6	24.2	303.8	5.9	9.9	15.3	-9.4	-57.8	
15.9	7.6	14.1	2.2	63.8	15.7	285.5	5.3	24.8	8.4	-7.4	-42.0	
29.0	7.2	87.5	8.4	81.0	18.1	336.7	126.8	54.7	11.3			
23.8	7.4	6.5	0.9	7.0	110.0	358.1	8.0	11.1	15.6	-5.8	-33.7	
18.3	7.4	6.5	1.0	116.0	8.0	367.2	8.5	10.2	17.2			
41.0	7.4	56.2	6.3	67.7	11.3	245.8	45.2	84.1	12.9	-7.4	-47.9	
51.0	7.3	195.5	20.2	38.7	5.6	472.8	113.4	3.3	19.4	-10.3	-63.2	

84.5	6.2	2756.1	81.9	773.6	124.7	384.3	6571.5	1287.2		-9.5	-59.8	
33.1	6.4	120.5	13.8	286.9	46.4	446.5	196.8	689.2	12.9	-7.9	-48.2	
15.2	7.0	17.2	2.6	73.2	10.8	196.4	21.8	83.8	5.4	-9.7	-59.6	
33.7	6.5	124.1	14.5	288.3	49.1	452.6	188.9	602.2	13.5	-7.4	-50.7	
56.6	6.6	67.1	18.0	350.3	48.3	241.6	71.7	1015.4		-8.9	-57.7	
62.2	6.8	68.4	18.1	361.3	52.5	242.2	77.1	1062.2		-9.1	-58.0	
8.6	8.1	0.6	0.2	44.3	13.5	205.6	0.6	7.1	2.1	-9.0	-53.0	
44.0	6.8	169.7	13.1	130.0	17.1	429.4	257.8	65.3	18.0	-9.5	-57.9	
9.0	7.9	7.1	1.0	44.2	4.6	178.7	3.7	9.3	2.6			
21.1	7.2	26.0	2.9	101.3	24.0	342.8	32.8	85.1	8.9	-9.4	-56.9	
20.0	9.0	450.0	16.0	4.1	0.0	565.5	301.6	17.0	7.1			
22.7	8.0	278.5	12.7	12.5	7.7	464.2	190.6	4.2	7.0			
26.5	7.2	65.9	5.6	145.0	40.2	230.0	41.9	479.2	12.4			
27.3	7.2	68.1	5.3	151.9	43.5	249.5	39.3	501.1	12.5			
35.0	7.3	33.6	3.0	39.9	25.6	328.2	11.9	1.8	13.9			
34.8	7.0	17.4	2.6	56.0	15.2	281.9	8.9	16.4	14.2			
20.0	7.2	13.3	2.6	67.7	31.0	311.0	23.3	40.1	26.7	-6.4	-31.1	Yuce G., Italiano F., D'Alessandro W., Yalcin T. H., Yasin D. U., Gulbay A. H., Ozyurt N. N., Rojay B., Karabacak V., Bellomo S., Brusca L., Yang T., Fu C. C., Lai C. W., Ozacar A. and Walia V. (2014) Origin and interactions of fluids circulating over the Amik Basin (Hatay, Turkey) and relationships with the hydrologic, geologic and tectonic settings. Chemical Geology 388, 23-39.
21.0	7.5	11.9	0.9	59.3	27.4	268.0	24.1	32.0	20.2	-6.5	-31.3	
21.0	7.2	42.6	1.0	55.0	106.0	580.0	60.8	89.9	32.3	-6.1	-29.8	
22.1	7.6	15.5	0.7	58.5	29.5	293.0	23.5	15.8	43.1	-5.6	-26.3	
22.6	7.4	16.0	1.3	60.7	37.1	329.0	25.2	37.2	28.8	-6.4	-31.7	
23.3	7.1	33.6	4.3	129.0	38.8	348.0	50.0	176.0	20.6	-6.0	-32.5	
29.0	7.3	24.8	4.7	94.3	30.2	305.0	39.3	78.5	20.7	-6.7	-36.6	
37.7	6.6	315.0	29.6	166.0	40.6	458.0	411.0	376.0	40.0	-7.0	-39.5	
25.8	6.9	27.2	1.3	87.2	18.4	317.0	36.5	27.8	27.2	-6.8	-36.7	
30.3	9.0	257.0	1.0	28.1	0.2	36.6	178.0	335.0	29.2	-7.1	-37.1	
28.9	7.1	28.5	3.6	87.1	66.0	390.0	47.1	101.0	45.4	-6.8	-35.5	

31.2	6.9	80.1	9.8	133.0	67.8	253.0	59.2	469.0	69.1	-6.6	-34.8
22.0	7.3	21.6	0.2	58.4	45.0	296.0	18.6	104.0	46.3	-6.8	-36.1
23.1	6.9	10.2	1.9	72.6	32.4	268.0	12.4	88.3	23.5	-7.3	-39.4
16.3	7.1	5.7	0.6	67.4	16.7	262.0	9.9	6.7	16.2	-7.2	-36.1
19.7	7.1	28.3	0.6	77.2	47.3	400.0	43.4	33.6	54.8	-6.4	-31.2
22.5	7.4	105.0	2.2	29.1	86.6	403.0	73.5	184.0	9.5	-4.6	-23.6
20.2		13.8	2.2	73.9	33.1	323.0	23.1	40.3	25.6	-5.9	-27.8
20.4		12.0	0.9	61.4	30.5	262.0	21.5	31.7	20.0	-5.9	-28.8
19.6		41.5	0.7	57.8	105.0	555.0	53.2	77.3	31.6	-5.9	-29.3
38.0	6.7	315.0	28.9	131.0	48.0	445.0	354.0	353.0	39.0	-6.7	-38.9
22.5	7.2	11.3	1.8	87.8	34.4	323.0	11.9	86.7	24.7	-6.8	-37.0
21.8	6.9	21.2	1.4	94.6	31.9	348.0	40.4	38.8	32.0	-6.3	-33.2
22.1	7.3	9.7	1.3	80.6	31.2	323.0	9.0	64.3	21.0	-7.2	-38.0
37.6	7.5	276.0	5.4	41.1	10.3	91.5	231.0	361.0	29.2	-7.2	-36.2
33.7	10.6	49.9	1.8	44.7	0.1	183.0	47.6	0.2	0.2	-8.7	-45.0
25.5	11.6	28.6	0.9	83.4	0.8	244.0	45.8	0.0	0.2	-7.9	-40.2
33.0	11.6	50.3	2.1	42.1	0.4	177.0	44.5	0.0	0.2	-8.1	-42.1
21.7	12.2	55.0	1.2	110.0	0.1	336.0	72.1	0.2	0.2	-7.9	-41.3
	6.3	0.8	0.2	3.6	0.2	13.0	1.6	4.4		-7.4	-40.0
	6.5	0.7	0.4	2.1	0.2	11.0	1.4	2.5		-7.7	-42.0
	6.7	0.7	0.3	2.3	0.2	5.0	1.4	3.8		-8.2	-46.0
		2.3	0.3	5.1	0.5	9.0	4.5	5.9		-4.5	-16.7
		2.2	0.4	3.9	0.4	15.0	4.2	4.1		-4.5	-18.7
		2.4	0.3	3.3	0.4	7.0	4.3	4.8		-6.1	-28.3

Note: The deep groundwater samples from Yuce et al. 2014 (sample ID: A4, A11, A4-2, A11-2, A38) were mixed with large amounts of seawater, so they were not used for simulation.

Table S2 Temperature results obtained with empirical chemical geothermometers (values in °C) and depths (km) of origin for EAFZ groundwaters.

No	T (°C)	Na-K			K-Mg	Li-Mg	Na-Li	Na-Ca	K-Ca	Na-K- Ca	SiO ₂			Circulation depth(km)
		a	b	c	d	e	f	g	k	i	j	k	l	
HS01	15.8	280.56	263.18	255.02	53.70	1164.31	115.33	113.53	167.74	177.81	64.74	76.87	32.72	1.8
HS02	13.2	44.69	32.02	14.64	340.90	794.35	58.83	-19.47	-23.39	16.11	19.81	35.51	-13.08	0.0
HS03	13.2	97.13	83.05	65.94	110.59	329.25	256.42	136.38	80.14	78.41	74.15	85.36	42.54	2.2
HS04	15.0	137.35	122.34	106.10	118.49	424.51	63.34	77.09	74.70	109.03	128.09	132.88	100.43	4.4
HS05	12.7	183.61	167.67	153.17	101.56	722.02	-11.79	69.20	92.54	139.57	51.58	64.90	19.12	1.3
HS06	15.0	211.67	195.23	182.19	117.90	1098.86	-23.85	43.82	87.06	149.16	53.76	66.89	21.36	1.4
HS07	9.8	24.22	12.15	-5.07	328.05	756.00	28.67	-0.77	-23.53	6.19	37.30	51.78	4.54	0.7
HS08	8.1	16.25	4.41	-12.71	326.88	752.56	17.37	8.17	-23.55	2.17	53.32	66.49	20.90	1.4
HS09	18.0	161.91	146.39	130.98	127.21	539.15	49.11	59.01	76.01	121.33	72.83	84.17	41.15	2.1
HS10	20.0	7.89	-3.69	-20.68	456.36	1200.82	5.80	38.91	-15.52	1.49	81.15	91.63	49.90	2.5
HS11	16.3	166.55	150.93	135.70	148.33	985.95	-6.80	27.09	57.05	113.61	38.24	52.65	5.49	0.8
HS12	16.9	0.78	-10.57	-27.44	436.27	1120.85	-3.85	56.07	-13.62	-1.56	98.46	107.00	68.28	3.2
HS13	18.2	232.80	216.03	204.29	97.49	530.50	52.80	54.40	103.32	166.87	39.42	53.74	6.69	0.8
HS14	23.5	226.40	209.73	197.58	48.47	350.37	216.09	188.63	187.64	224.53	87.85	97.61	56.98	2.7
HS15	32.0	150.02	134.74	118.90	26.34	286.57	170.79	210.97	148.15	176.18	-39.83	-21.62	-71.20	
HS16	24.5	299.42	281.83	275.35	25.48	540.78	122.71	258.29	274.78	375.41	82.83	93.13	51.67	2.5

Note: Circulation depth(km) = (T-T₀)/g+h. “T” is reservoir temperature estimated by SiO₂. “T₀” is annual average temperature in EAFZ is 20 °C. “g” is geothermal gradient is ~2.50 °C/100 m. “h” is thickness of the constant temperature zone is 30 m.

a Na-K, $T = 1390 / [\log(\text{Na/K}) + 1.75] - 273.15$ (Giggenbach, 1988).

b Na-K, $T = 933 / [\log(\text{Na/K}) + 0.993] - 273.15$ (Arnórsson, 1983).

c Na-K, $T = 1178 / [\log(\text{Na/K}) + 1.47] - 273.15$ (Nieva and Nieva, 1987).

d K-Mg, $T = 4410 / [\log(\text{K/Mg}^{1/2}) + 14.0] - 273.15$ (Giggenbach, 1988).

e Li-Mg, $T = 2200 / [\log(\text{Li/Mg}^{1/2}) + 5.47] - 273.15$ (Kharaka and Mariner, 1989).

f Na-Li, $T = 1000 / [\log(\text{Na/Li}) + 0.389] - 273.15$ (Fouillac and Michard, 1981).

g Na-Ca, $T = 1096.7 / [3.08 - \log(\text{Na/Ca}^{1/2})] - 273.15$ (Tonani, 1980).

h K-Ca, $T = 1930 / [3.861 - \log(\text{K/Ca}^{1/2})] - 273.15$ (Tonani, 1980).

i Na-K-Ca, $T = 1647 / [\log(\text{Na/K}) + 1/3\log(\text{Ca}^{1/2}/\text{Na}) + 2.24] - 273.15$ (Fournier and Truesdell, 1973).

j Quartz, no steam loss, $T = 1309 / [5.19 - \log(\text{SiO}_2)] - 273.15$ (Fournier, 1977).

k Quartz, maximum steam loss, $T = 1522 / [5.75 - \log(\text{SiO}_2)] - 273.15$ (Fournier, 1977).

l Chalcedony, $T = 1032 / [4.78 - \log(\text{SiO}_2)] - 273.15$ (Fournier, 1977).

Part S4:

Videos:

Video. 1 Seismic precursor anomaly of HS14 geothermal fluid. See Supporting Information Video. 1.

Video. 2 Post-earthquake anomaly of HS04 geothermal fluid. See Supporting Information Video. 2.

References

- Arnórsson, S.: Chemical equilibria in icelandic geothermal systems—Implications for chemical geothermometry investigations, *Geothermics*, 12, 119-128, [https://doi.org/10.1016/0375-6505\(83\)90022-6](https://doi.org/10.1016/0375-6505(83)90022-6), 1983.
- Aydin, H., Karakuş, H., and Mutlu, H.: Hydrogeochemistry of geothermal waters in eastern Turkey: Geochemical and isotopic constraints on water-rock interaction, *Journal of Volcanology and Geothermal Research*, 390, 10.1016/j.jvolgeores.2019.106708, 2020.
- Baba, A., Şaroğlu, F., Akkuş, I., Özel, N., Yeşilnacar, M. İ., Nalbantçılar, M. T., Demir, M. M., Gökçen, G., Arslan, Ş., Dursun, N., Uzelli, T., and Yazdani, H.: Geological and hydrogeochemical properties of geothermal systems in the southeastern region of Turkey, *Geothermics*, 78, 255-271, <https://doi.org/10.1016/j.geothermics.2018.12.010>, 2019.
- Fouillac, C. and Michard, G.: Sodium/lithium ratio in water applied to geothermometry of geothermal reservoirs, *Geothermics*, 10, 55-70, [https://doi.org/10.1016/0375-6505\(81\)90025-0](https://doi.org/10.1016/0375-6505(81)90025-0), 1981.
- Fournier, R. O.: Chemical geothermometers and mixing models for geothermal systems, *Geothermics*, 5, 41-50, [https://doi.org/10.1016/0375-6505\(77\)90007-4](https://doi.org/10.1016/0375-6505(77)90007-4), 1977.
- Fournier, R. O. and Truesdell, A. H.: An empirical Na-K-Ca geothermometer for natural waters, *Geochimica Et Cosmochimica Acta*, 37, 1255-1275, 1973.
- Giggenbach, W. F.: Geothermal solute equilibria. Derivation of Na-K-Mg-Ca geothermometers, *Geochimica et Cosmochimica Acta*, 52, 2749-2765, [https://doi.org/10.1016/0016-7037\(88\)90143-3](https://doi.org/10.1016/0016-7037(88)90143-3), 1988.
- Giggenbach, W. F.: *Chemical Techniques in Geothermal Exploration, Application of Geochemistry in Geothermal Reservoir Development*, 1991.
- Italiano, F., Sasmaz, A., Yuce, G., and Okan, O. O.: Thermal fluids along the East Anatolian Fault Zone (EAFZ): Geochemical features and relationships with the tectonic setting, *Chemical Geology*, 339, 103-114, 10.1016/j.chemgeo.2012.07.027, 2013.
- Karaoğlu, Ö., Bazargan, M., Baba, A., and Browning, J.: Thermal fluid circulation around the Karliova triple junction: Geochemical features and volcano-tectonic implications

- (Eastern Turkey), *Geothermics*, 81, 168-184, 10.1016/j.geothermics.2019.05.003, 2019.
- Karaoğlu, Ö., Gülmez, F., Göçmengil, G., Lustrino, M., Di Giuseppe, P., Manetti, P., Savaşçın, M. Y., and Agostini, S.: Petrological evolution of Karlıova-Varto volcanism (Eastern Turkey): Magma genesis in a transtensional triple-junction tectonic setting, *Lithos*, 364-365, 10.1016/j.lithos.2020.105524, 2020.
- Kharaka, Y. K. and Mariner, R. H.: Chemical Geothermometers and Their Application to Formation Waters from Sedimentary Basins, *Thermal History of Sedimentary Basins*, New York, NY, 1989//, 99-117,
- Nieva, D. and Nieva, R.: Developments in geothermal energy in Mexico—part twelve. A cationic geothermometer for prospecting of geothermal resources, *Heat Recovery Systems and CHP*, 7, 243-258, [https://doi.org/10.1016/0890-4332\(87\)90138-4](https://doi.org/10.1016/0890-4332(87)90138-4), 1987.
- Nurlu, N.: Geochronological, Geochemical and Sr-Nd-Pb Isotope Characteristics of the Meydan Ophiolite, SE Turkey: Petrogenesis and Implications for Mesozoic Tectonic Evolution, *Geochemistry International*, 58, 639-669, 10.1134/s0016702920060099, 2020.
- Okan, O. O., Kalender, L., and Cetindag, B.: Trace-element hydrogeochemistry of thermal waters of Karakocan (Elazig) and Mazgirt (Tunceli), Eastern Anatolia, Turkey, *Journal of Geochemical Exploration*, 194, 29-43, 10.1016/j.gexplo.2018.07.006, 2018.
- Parkhurst, D. L. and Appelo, C. A. J.: Description of input and examples for PHREEQC version 3: a computer program for speciation, batch-reaction, one-dimensional transport, and inverse geochemical calculations, *Techniques and Methods*, 6-A43, U.S. Geological Survey, Reston, VA, 10.3133/tm6A43, 2013.
- Pasvanoglu, S.: Geochemistry and conceptual model of thermal waters from Ercis - Zilan Valley, Eastern Turkey, *Geothermics*, 86, 10.1016/j.geothermics.2020.101803, 2020.
- Tonani, F. B.: Some Remarks on the Application of Geochemical Techniques in geothermal exploration, *Advances in European Geothermal Research*, 428-443, https://doi.org/10.1007/978-94-009-9059-3_38, 1980.
- YASİN, D. and YÜCE, G.: Isotope and hydrochemical characteristics of thermal waters along the active fault zone (Erzin-Hatay/Turkey) and their geothermal potential, *Turkish Journal of Earth Sciences*, 32, 721-739, 10.55730/1300-0985.1871, 2023.

Yuce, G., Italiano, F., D'Alessandro, W., Yalcin, T. H., Yasin, D. U., Gulbay, A. H., Ozyurt, N. N., Rojay, B., Karabacak, V., Bellomo, S., Brusca, L., Yang, T., Fu, C. C., Lai, C. W., Ozacar, A., and Walia, V.: Origin and interactions of fluids circulating over the Amik Basin (Hatay, Turkey) and relationships with the hydrologic, geologic and tectonic settings, *Chemical Geology*, 388, 23-39, 10.1016/j.chemgeo.2014.09.006, 2014.